Spectra and binding energy predictions of chiral interactions for ^{7}Li

A. Nogga,[1,*] P. Navrátil,[2,†] B. R. Barrett,[3,‡] and J. P. Vary[4,2,5,§]

[1]*Institut für Kernphysik, Forschungszentrum Jülich, D-52425 Jülich, Germany*
[2]*Lawrence Livermore National Laboratory, L-14, P.O. Box 808, Livermore, California 94551, USA*
[3]*Department of Physics, University of Arizona, Tucson, Arizona 85721, USA*
[4]*Department of Physics and Astronomy, Iowa State University, Ames, Iowa 50011, USA*
[5]*Stanford Linear Accelerator Center, Stanford University, Stanford, California 94309, USA*

Using the no-core shell model approach, we report on the first results for ^{7}Li based on the next-to-next-to-leading order chiral nuclear interaction. Both two-nucleon and three-nucleon interactions are taken into account. We show that the p-shell nuclei are sensitive to the subleading parts of the chiral interactions including three-nucleon forces. Though chiral interactions are soft, we do not observe overbinding for this p-shell nucleus and find a realistic description for the binding energy, excitation spectrum, and radius.

PACS number(s): 21.10.−k, 21.30.−x, 27.20.+n, 21.60.−n

I. INTRODUCTION

We are currently experiencing rapid progress in our understanding of nuclear properties. This is triggered by two major developments.

On one hand, we have increasingly powerful supercomputers, for which new and very efficient algorithms have been developed to solve the nuclear many-body problem. We are now able to solve the Schrödinger equation for realistic nuclear interactions for p-shell nuclei, including also three-nucleon forces (3NFs) [1,2]. This is a major advance in itself, because it is becoming more clear that reliable predictions for many nuclear observables, binding energy, and spectra can be obtained from phenomenological nuclear two- (NN) and three-nucleon ($3N$) interaction models. Especially, for the NN system, these have reached a high degree of sophistication and describe the NN data up to pion production threshold perfectly [3–6]. For the binding energies of p-shell nuclei, the structure of the 3NFs turned out to be significant, leading to improved models of these forces engineered to describe a wide range of light nuclei accurately [7]. This tool is of increasing importance to determine, e.g. reaction rates for astrophysical processes [8], which are experimentally not accessible or properties of nuclei with large neutron excess [1].

On the other hand, there was a great deal of progress in our understanding of how chiral perturbation theory (ChPT) can be extended from purely pionic or the nucleon-pion system (for a review see, e.g. [9]) to systems with more than one nucleon [10–12]. In this approach, one makes use of the explicit and spontaneous breaking of chiral symmetry to systematically expand the strong interaction in terms of a generic small momentum. Thereby, the NN interactions, the 3NFs and πN scattering are related to each other. The chiral symmetry and the pattern of its breaking are not systematically taken into account by today's phenomenological interactions, except that in all of them the longest-range part of the potential is generally the one-pion-exchange interaction. Therefore, though QCD is believed to be the theory of the strong interaction for the energies of relevance in nuclear systems, we are not able to perform confirming tests using the traditional forces. This will be possible using nuclear forces based on ChPT. It will be especially important to look at subleading parts of the interaction, which include the 2π exchange NN and $3N$ forces. Here, many of the relations between NN, $3N$, and πN interactions become apparent. Therefore, finding signatures of the 3NFs is an important aspect of current research on this issue.

In the past, the effects of 3NFs have been studied using the phenomenological models. In nucleon-deuteron (Nd) scattering above 60–100 MeV lab energy, it was found that predictions for some (polarization) observables depend on the 3NF model used but not on the NN interaction chosen [13]. These observables are excellent candidates to pin down the structure of 3NFs and, therefore, outstanding laboratories to study the important subleading parts of the chiral interactions. Consequently, a lot of experiments were triggered, which provide an important set of data to probe these models [14–17]. First comparisons for chiral interactions to the data were performed and, in general, agreement was found in the energy range, where chiral interactions are expected to work [18].

These data, however, are manifestly isospin $T = 1/2$ and, therefore, not suitable to probe the 3NF in the isospin $T = 3/2$ channel. But it was argued that the $T = 3/2$ component is very important to describe p-shell nuclei, which mainly motivated the new 3NF terms in the Illinois series of $3N$ interactions [7]. This clearly shows that the spectra and binding energies of light nuclei are complementary to nd scattering and provide indispensable information on the structure of 3NFs. It is therefore of utmost importance to predict properties of p-shell nuclei based on the chiral interactions including these 3NFs.

Chiral interactions are low-momentum interactions. The unknown short distance part of the force is absorbed in a tower of contact terms. Necessarily, we need to regularize the

---

*Electronic address: a.nogga@fz-juelich.de
†Electronic address: navratil1@llnl.gov
‡Electronic address: bbarrett@physics.arizona.edu
§Electronic address: jvary@iastate.edu

interactions with cutoff functions. It turns out that one obtains a decent description of the NN data using rather small cutoffs. This is advantageous, because the resulting interactions are soft and convergence is generally faster than the convergence with traditional models. But this has also been criticized in the past. The experience with traditional models indicated a need for rather hard cores not only in the NN interaction but also in the 3NF to prevent strong overbinding in systems beyond the s shell. This is a surprising result, because it means that we cannot properly separate high energy degrees of freedom from the low energy part. Because the high momentum tail of traditional interactions is strongly model dependent, a sensitivity to this tail will induce a strong model dependence of the results. Indeed, the binding energies of nuclei do depend on the chosen NN interaction model. It is believed that this model dependence is strongly reduced, once 3NFs consistent with the NN force are added (in fact it was proven that any NN interaction can be augmented by a 3NF so that the description of the $3N$ data is identical to that of a second phase-equivalent NN force [19], thereby removing the model dependence). Similarly, one can expect that a consistent combination of NN and $3N$ force will lead to a reasonable description of light nuclei even if the high momentum tail is completely missing. An important aspect of this work will be to confirm this expectation by an explicit calculation.

Because of the strong nonlocality of today's chiral interactions, to the best of our knowledge, there is only one reliable many-body technique to solve the Schrödinger equation for p-shell nuclei for these interactions including the 3NFs. This is the *ab initio* no-core shell model (NCSM) [2,20,21]. In this article, we use the NCSM to predict spectra and binding energies for ^{7}Li. These results will be presented along with calculations for the s-shell states for ^{3}H and ^{4}He, which were used to determine unknown parameters of the 3NF. The p-shell results are then predictions.

The manuscript is organized as follows. In Sec. II, we start with a brief summary of the status on the research on chiral interaction models, mainly to explain the force model entering in the calculations. The NCSM approach is introduced in Sec. III to keep this article self-contained. Then, in Sec. IV, we discuss our numerical results. Conclusions and an outlook will be given in Sec. V.

II. CHIRAL INTERACTIONS

Microscopic nuclear structure is generally based on NN interactions, which describe the NN scattering data up to π-production threshold perfectly. Usually, such interactions are based on the 1π exchange, which is augmented by a more or less phenomenological short-range part. It turns out that binding energies based on these interactions are model dependent and too small [1,22,23]. 3NFs are clearly necessary.

However, defining consistent combinations of NN and $3N$ forces is not a trivial task, and rarely are both based on a single underlying theory. In practice, the NN interaction models are usually augmented by a 2π exchange 3NF [24,25] or extended versions thereof [7]. Then parameters are mostly adjusted to reproduce the binding energies of s-shell nuclei or nuclear

matter density. Though this can be very successful in the description of nuclear properties [7], it lacks a solid theoretical foundation. The relation to quantum chromodynamics (QCD) is completely lost. Processes of other strongly interacting systems, like the πN system, are not quantitatively related to these forces, though the basic mechanisms involve these particles.

Because lattice simulations for nuclei are not realistic for the foreseeable future, effective field theory is an appealing theoretical foundation on which to build. In its simplest form, an effective field theory was formulated that explicitly takes only nucleons into account. It is accompanied by a power counting in terms of powers of r/a, where r is the effective range of the interaction and a the large scattering length of the NN system (for a recent review see Ref. [26]). This property is realized in very different physical systems, e.g., ^{4}He clusters and atoms close to a Feshbach resonance. It allows one to identify universal properties. Also, it is possible to identify nuclear properties, which are dominated by the large scattering length of the NN interaction. An example is the correlation between ^{3}H and ^{4}He binding energies, known as Tjon-line, which is naturally explained using this approach [27]. Although these results are interesting in themselves, they are by construction not that interesting for the relation of quantum chromodynamics (QCD) and nuclear physics. The approach will describe only observables, which do not reflect any specific property of QCD except the large scattering length.

To sense the leading role of QCD, another effective field theory is the tool of choice: ChPT. The new physical input is the approximate chiral symmetry of QCD, which is known to be spontaneously broken. Based on this an effective field theory can be formulated that involves nucleons and πs explicitly. The Goldstone-boson character of the πs (related to the spontaneous breaking of chiral symmetry) guarantees that amplitudes in purely pionic and the πN system can be expanded in powers of a small, typical momentum Q. The explicit breaking of chiral symmetry because of the finite quark masses is expanded similarly in terms of the π mass [28]. Electromagnetic effects on the quark level and quark mass differences have also been taken into account by an expansion of isospin symmetry breaking contributions in terms of the fine structure constant and the quark mass differences [29,30].

Obviously, the NN system is different. The deuteron bound state clearly shows that a perturbative treatment is impossible. Weinberg realized that this is understood by an enhancement of reducible diagrams in two- or more-nucleon systems and proposed to expand the irreducible diagrams perturbatively in terms of small external momenta, but then sum all these diagrams to infinite order using a Lippmann-Schwinger or Schrödinger equation [31,32]. In other words, Weinberg suggested to obtain nuclear potentials from ChPT. This naturally explains that NN interactions are much more important than 3NFs and that these are more relevant than higher-body interactions [33]. The approach was quantitatively confirmed [34–36]. For the NN system, terms up to order momentum Q^4 have been taken into account nowadays [37,38] and lead to a description of NN data, which is comparable to the one of the phenomenological interactions. The approach

to sum all irreducible diagrams to infinite order is usually called "Weinberg counting." Other schemes to deal with the nonperturbativity have been proposed [39] and are formally more consistent, because the renormalization is understood analytically. But the formal problems of the "Weinberg" scheme, which were pointed out in Ref. [39], can be circumvented by small cutoffs of the order of 500 MeV for the regularization of the Lippmann-Schwinger equation. Under this condition, "Weinberg power-counting" is numerically more successful than the scheme of Ref. [39], as was shown in Ref. [40]. Indirect confirmation of the Weinberg approach is the favorable agreement of parameters extracted from πN scattering [41] and an NN phase-shift analysis [42,43]. Therefore, for the rest of this article, we will rely on the Idaho-N3LO interaction [37] based on "Weinberg counting" for the NN interaction. It takes terms up to order Q^4 into account and is able to describe the NN-scattering data below π-production threshold perfectly. We stress that this can only be a first step, because a complete analysis of the chiral interactions requires further order-by-order analysis to confirm convergence.

Very soon the leading 3NFs, which appear at order Q^3 were derived [44]. They consist of a 2π exchange term, which is very similar to the widely used Tucson-Melbourne 3NF [25] and, additionally, there are contact interactions with and without 1π exchange. In the original article, five such contact terms were believed to be independent. Fortunately, it turned out later, that only two of them remain independent once the identity of the nucleons is taken into account. In this simplified form the 3NFs were applied to Nd scattering, the ^{3}H and ^{4}He bound states [18]. For completeness, the explicit expressions for these forces are given in Appendix A.

For the 2π-exchange term, the power of this systematic scheme to derive consistent NN and $3N$ interactions comes into play. All vertices also occur in NN interaction diagrams. This completely determines the strength and form of this part of the 3NF. As outlined in the appendix, there are three less-well-known strength constants in this part of the 3NF: c_1, c_3, and c_4. They determine the contribution of various spin-isospin structures to the off-shell πN-scattering amplitude entering the 3NF. Table I summarizes the results of recent determinations of these constants. The most fundamental determinations were done in Ref. [41,45] using a fit to πN-scattering data. For this system, ordinary ChPT without resummation is used. The possibility to extract these constants from πN data makes the strong link of the nuclear interaction and other strong interaction processes in ChPT explicit. The rather scarce set

of data for the πN system induces rather large uncertainties. This has partly been circumvented in [41] using dispersion relations. Therefore, the determination of Ref. [41] is usually considered to be more accurate, though this is not reflected in the estimates of the uncertainty, which we simply repeat from the original work in the table. It is nice to see that this result compares very well with the determination of [42,46], where the c_is were extracted from a partial-wave analysis of NN data. For the Idaho-N3LO interaction, the authors of [37] preferred their own determination for c_3 and c_4 based on a fit to phase shifts in high partial waves, also shown in the table. It slightly deviates from the two previous values and led to an intense debate on the correct way to extract these constants from NN data. We cannot contribute to this discussion but use the c_is of [37], simply because we want consistency of the NN and $3N$ forces. The exact magnitude of these constants should be of less importance, because they only appear in subleading terms of minimal order Q^3. However, this issue has to be kept in mind, when we compare our results to the experimental values, especially for observables, where 3NFs are important. Please note that we combine an NN interaction of order Q^4 to a 3NF of order Q^3 only. Because we will not study the convergence of our predictions with respect to the chiral expansion in this work, we think that this combination is justified. It is the state-of-the-art for chiral interaction models.

For the remaining two contact 3NFs, two more strength constants enter: c_D and c_E (see the appendix for the definition). In Ref. [18], it was shown that the determination of these constants is possible by a fit to the ^{3}H binding energy and the Nd doublet scattering length. This is only one of the possibilities to determine these constants. For the Idaho-N3LO force, we therefore decided to fit to the ^{3}H and ^{4}He binding energies. For our study here, this has two advantages. First, a very accurate fit is possible, because both binding energies are well known experimentally. Second, it makes a comparison of our results to calculations with the phenomenlogical model AV18/Urbana-IX more meaningful, because this combination describes both binding energies reasonably well but fails for some p-shell spectra. The fit was performed using Faddeev-Yakubovsky calculations. For a detailed description of the technique, we refer to Ref. [22]. Using the ^{3}H binding energy, we established a relation between c_D and c_E, shown in Fig. 1. For all these combinations of c_D and c_E, Idaho-N3LO in combination with the 3NF predict a ^{3}H binding energy of 8.482 MeV in agreement with experiment. These combinations then enter in a calculation of the Yakubovsky eigenvalue η for ^{4}He using the α particle binding energy of 28.3 MeV as trial energy. Our theoretical prediction agrees with 28.3 MeV, if η is equal to 1. From the results shown in Fig. 2, we can read off that two combinations of c_D and c_E describe ^{3}H and ^{4}He equally well. For later reference, we call them 3NF-A and 3NF-B. The numerical values are listed in Table II.

We did not perform complete calculations for the binding energy for ^{4}He for each combination of c_D and c_E. However, generally, one can expect from the ranges of η results that the binding energy would change by approximately 2 MeV in the range of c_Ds considered. This sets a scale for the Q^3 contribution to ^{4}He. For completeness, we also note that the pp force was augmented by the Coulomb interaction for point like

TABLE I. Various determinations of the strength constants c_i of the 3NF. All values are in GeV^{-1}.

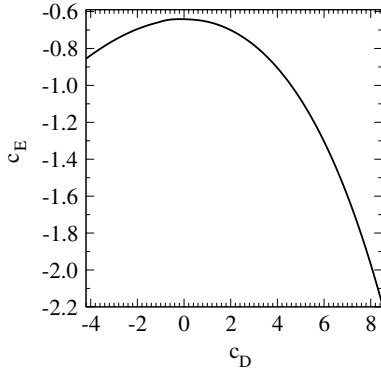|	c_1	c_3	c_4
Fettes *et al.* [45]	-1.23 ± 0.16	-5.94 ± 0.09	3.47 ± 0.05
Büttiker *et al.* [41]	-0.81 ± 0.15	-4.69 ± 1.34	3.40 ± 0.04
Rentmeester *et al.* [46]	-0.76 ± 0.07	-5.08 ± 0.28	4.70 ± 0.70
Rentmeester *et al.* [42]	-0.76 ± 0.07	-4.78 ± 0.10	3.96 ± 0.22
Entem *et al.* [37]	-0.81	-3.20	5.40

FIG. 1. Correlation of the two dimensionless strength constants c_D and c_E of the 3NF. All combinations of c_D and c_E describe the ^{3}H binding energy equally well.

protons. No further electromagnetic contribution was taken into account as they are expected to be of less importance. We also do not include the first relativistic corrections to the 3NF, which some people do count as an order Q^3 contribution. We cannot discuss this issue here. We claim only that whatever counting you prefer, the relativistic corrections will be smaller than our Q^3, because we use cutoffs around 500 MeV, which are much smaller than the nucleon mass. Then, because no four-nucleon forces enter at order Q^3, our interaction is complete up to this order. Now we need to extend our calculations to the p shell. For this, we give a brief introduction to the NCSM in the next section.

III. NCSM APPROACH

Usually shell-model calculations exploit the possibility to assume an inert nuclear core. Taking only the valence nucleons as active particles clearly has the advantage to keep the number of many-nucleon states manageable, but, so far, it also means that effective shell-model interactions have to be used, which cannot be related directly to nuclear interactions, as they have been developed for few-nucleon systems. The *ab initio* NCSM is different [20,21]. Because all nucleons are taken to be active, in principle, the same interactions can be used for the
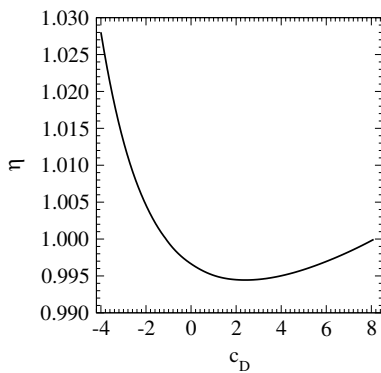

FIG. 2. Eigenvalues η of the Yakubovsky equations for ^{4}He depending on c_D. c_E is chosen according to Fig. 1. $\eta = 1$ corresponds to describing the ^{4}He binding energy exactly.

TABLE II. Combinations of c_D and c_E, which describe the ^{3}H and ^{4}He binding energies.

	c_D	c_E
3NF-A	-1.11	-0.66
3NF-B	8.14	-2.02

NCSM as for traditional few-body calculations. However, for realistic nuclear forces, the wave function is hardly described by combinations of single-particle states. Using harmonic oscillator (HO) states, which allow for an easy separation of the center-of-mass (c.m.) motion from the internal degrees of freedom, one encounters the additional problem to describe the the exponential long range tail of the wave function. Again effective interactions become necessary to achieve convergence, with a small number of HO states taken into account. These effective interactions are systematically related to the "bare" interactions [47,48].

The scheme described in Ref. [48] is based on unitary transformations of the Hamiltonian [49], which decouples the model space from the complete Hilbert space describing the quantum mechanical system. Such transformations have already proven to be useful in a wide variety of nuclear physics problems. They allow us to decouple parts of the Fock space, such as the two nucleon space, from the rest of the Fock space [50]. Also a decoupling of low- and high-momentum components has been performed using the same approach [51,52]. In many-body problems, it has not only been used for shell-model calculations, but, recently, could be exploited for the solution of nuclear problems in the hyperspherical harmonics basis [53,54].

The starting point of all NCSM calculations is a non-relativistic A-body Hamiltonian, which includes NN and, important here, $3N$ interactions

$$H_A = \sum_{i=1}^{A} \frac{\vec{p}_i^{\,2}}{2m_i} + \sum_{i<j=1}^{A} V_{ij} + \sum_{i<j<k=1}^{A} V_{ijk}, \quad (1)$$

where $\vec{p}_i$ are the momenta of the A particles with masses m_i. In the following, we assume that the interaction does not change the type of particle and that the total mass $M_A = \sum_i m_i$ is well defined. Adding the c.m. HO potential, one can rewrite the Hamiltonian as [55]

$$
\begin{aligned}
H_A^\Omega = H_A + \frac{M_A \Omega^2}{2} \vec{R}^2 &= \sum_{i=1}^{A} \left(\frac{\vec{p}_i^{\,2}}{2m_i} + \frac{m_i \Omega^2}{2} \vec{r}_i^{\,2} \right) \\
&+ \sum_{i<j=1}^{A} \left[V_{ij} - \frac{m_i m_j}{2M_A} \Omega^2 (\vec{r}_i - \vec{r}_j)^2 \right] + \sum_{i<j<k=1}^{A} V_{ijk},
\end{aligned}
$$

$$(2)$$

with the c.m. position $\vec{R} = \frac{1}{M_A} \sum_i m_i \vec{r}_i$.

In the following we try to establish an unitary tranformation of the Hamiltonian, which decouples two parts of the Hilbert space. A rather small finite model space P and the rest of the Hilbert space Q. The projection operators on the two spaces are also called P and Q. They fulfill the relation $Q = 1 - P$.

Okubo [49] showed that the unitary operator can be derived from an operator ω, which fulfills the following relations:

$$\omega = Q\omega P \tag{3}$$

$$0 = Qe^{-\omega}H_A^\Omega e^{+\omega}P$$
$$= Q(1-\omega)H_A^\Omega(1+\omega)P. \tag{4}$$

The transformation e^ω already decouples the subspaces P and Q, but it is not unitary. Unitarity can be achieved using the anti-Hermitian operator $S = \text{arctanh}(\omega - \omega^\dagger)$ and defining the unitary operator $U = e^{+S}$. Using the properties of S and ω, one finds the explicit expression [49]

$$U = e^S = (1 + \omega - \omega^\dagger)(1 + \omega\omega^\dagger + \omega^\dagger\omega)^{-1/2}. \tag{5}$$

The problem is reduced to finding the operator ω. For that, one defines a set of d_P eigenstates $|n\rangle$ of the Hamilton operator H_A^Ω, where d_P is the dimension of the model space P. Defining $\omega|n\rangle \equiv Q|n\rangle$, it is easy to show that the decoupling condition Eq. (4) holds. This completely defines the ω operator for sets of eigenstates $|n\rangle$, for which the $P|n\rangle$ are linearly independent. In practice, for resonable choices of the eigenstates, this condition is always fulfilled. Using Eq. (3) the action of ω on $|n\rangle$ reads

$$\langle\alpha_Q|n\rangle = \sum_{\alpha_P}\langle\alpha_Q|\omega|\alpha_P\rangle\langle\alpha_P|n\rangle$$
$$\equiv \sum_{\alpha_P}\langle\alpha_Q|\omega|\alpha_P\rangle N_{\alpha_P n}, \tag{6}$$

where α enumerates the basis states. The indices P and Q restrict enumeration to the respective subspace. With the help of the inverse $M = N^{-1}$, the matrix elements of ω are found [56] easily in a noniterative scheme

$$\langle\alpha_Q|\omega|\alpha_P\rangle = \sum_n \langle\alpha_Q|n\rangle M_{n\alpha_P}. \tag{7}$$

As elaborated in Ref. [57], there is always as set of states $|n\rangle$, for which the inverse of N exists. In practice, one chooses the d_P lowest lying eigenstates of H_A^Ω. Because $(1 - \omega + \omega^\dagger)|n\rangle$ has only P-space components, the same holds for $U^\dagger|n\rangle$. Matrix elements of states $|n\rangle$ are then exactly reproduced in the model space

$$\langle n'|O|n\rangle = \langle n'|U \underbrace{PU^\dagger OUP}_{O_{\text{eff}}} U^\dagger|n\rangle. \tag{8}$$

Because we are interested only in the P-space matrix elements of O_{eff}, we can make use of the simplification

$$UP = (1+\omega)(1+\omega^\dagger\omega)^{-1/2}P \tag{9}$$

and write

$$\langle\alpha_P|O_{\text{eff}}|\beta_P\rangle = \sum_{\alpha_P'\beta_P'}\langle\alpha_P|(1+\omega^\dagger\omega)^{-1/2}|\alpha_P'\rangle$$
$$\times \sum_{nn'}M_{n\alpha_P'}^*M_{n'\beta_P'}\langle n|O|n'\rangle$$
$$\times \langle\beta_P'|(1+\omega^\dagger\omega)^{-1/2}|\beta_P\rangle. \tag{10}$$

Here we made use of the relation

$$\langle\alpha_P|(1+\omega^\dagger)O(1+\omega)|\beta_P\rangle$$
$$= \sum_{nn'}M_{n\alpha_P}^*M_{n'\beta_P}\langle n|O|n'\rangle. \tag{11}$$

There are two special cases of interest of Eq. (11). The first, $O = 1$, is useful to determine the P-space renormalization operator $(1+\omega^\dagger\omega)^{-1/2}$ because

$$\langle\alpha_P|(1+\omega^\dagger)(1+\omega)|\beta_P\rangle = \langle\alpha_P|(1+\omega^\dagger\omega)|\beta_P\rangle$$
$$= \sum_n M_{n\alpha_P}^*M_{n\beta_P}. \tag{12}$$

The second, $O = H_A^\Omega$, makes the evaluation of the effective Hamiltonian especially simple

$$\langle\alpha_P|\mathcal{H}_{\text{eff}}|\beta_P\rangle = \langle\alpha_P|(1+\omega^\dagger)H_A^\Omega(1+\omega)|\beta_P\rangle$$
$$= \sum_n M_{n\alpha_P}^*M_{n\beta_P}E_n, \tag{13}$$

with E_n the eigenenergies of the eigenstates $|n\rangle$. These equations are exact. They reduce the problem to one in a very small model space P. However, because solutions of the problem are necessary to obtain the effective operator, they do not help to solve the eigenvalue problem in this form.

The NCSM concept becomes useful by approximating the effective interaction in an a-body cluster approximation. There are two obvious constraints on this approach. First, to keep the approximation controllable, we require that the effective interaction approaches the bare interaction for model spaces $P \to \infty$, and, second, we expect best convergence, when the nuclear part of the interaction acts in the a-body cluster with the same strength as in a free a-body system. Then, under the assumption that only $b = 2$-body bare forces contribute, one needs to solve the cluster problem for

$$H_a^\Omega = \sum_{i=1}^a\left(\frac{\vec{p}_i^{\,2}}{2m_i} + \frac{m_i\Omega^2}{2}\vec{r}_i^{\,2}\right)$$
$$+ \sum_{i<j=1}^a\left[V_{ij} - \frac{m_im_j}{2M_A}\Omega^2(\vec{r}_i - \vec{r}_j)^2\right]. \tag{14}$$

Note that in this cluster Hamiltonian, the strength of the HO two-body potential depends on the original A. This induces a confining meanfield potential for the cluster, which simply reflects that the cluster is embedded in the nuclear environment. It has the nice property that we can base our effective interaction on an infinite set of cluster bound states. No scattering states need to be considered. The effective interaction for b-body interactions in the a-body cluster approximation for the A-body system is defined as

$$\mathcal{V}_{\text{eff}}^{A,a,b} = \mathcal{H}_{\text{eff}} - \sum_{i=1}^a\left(\frac{\vec{p}_i^{\,2}}{2m_i} + \frac{m_i\Omega^2}{2}\vec{r}_i^{\,2}\right), \tag{15}$$

where $\mathcal{H}_{\text{eff}}$ is derived from an Hamiltonian operator like given in Eq. (14). The effective interaction enters into the A-body problem with a different weight, that insures that the bare

interaction is recovered for large model spaces [20,21]

$$\mathcal{H}_{\text{eff}}^A = \sum_{i=1}^A \left(\frac{\vec{p}_i^{\,2}}{2m_i} + \frac{m_i\Omega^2}{2}\vec{r}_i^{\,2} \right)$$
$$+ \frac{(A-a)!(a-b)!}{(A-b)!} \sum_{i_1 < i_2 \ldots < i_a = 1}^A \mathcal{V}_{\text{eff},i_1\ldots i_a}^{A,a,b}. \quad (16)$$

In this form it becomes apparent that we have a double counting problem, when both $b = 2$ and $b = 3$ interactions enter the cluster Hamiltonian. This can be solved as outlined in [2] and requires two effective interactions. The first one, $\mathcal{V}_{\text{eff},i_1\ldots i_a}^{A,a,NN}$, is based on the Hamiltonian in Eq. (14). The second one, $\mathcal{V}_{\text{eff},i_1\ldots i_a}^{A,a,3N}$, is based on

$$H_a^\Omega = \sum_{i=1}^a \left(\frac{\vec{p}_i^{\,2}}{2m_i} + \frac{m_i\Omega^2}{2}\vec{r}_i^{\,2} \right)$$
$$+ \sum_{i<j=1}^a \left[V_{ij} - \frac{m_i m_j}{2M_A}\Omega^2(\vec{r}_i - \vec{r}_j)^2 \right]$$
$$+ \sum_{i<j<k=1}^a V_{ijk}, \quad (17)$$

which additionally takes into account the 3NF. The combination

$$\mathcal{H}_{\text{eff}}^A = \sum_{i=1}^A \left(\frac{\vec{p}_i^{\,2}}{2m_i} + \frac{m_i\Omega^2}{2}\vec{r}_i^{\,2} \right)$$
$$+ \frac{(A-a)!(a-3)!}{(A-3)!} \sum_{i_1 < \ldots < i_a = 1}^A \mathcal{V}_{\text{eff},i_1\ldots i_a}^{A,a,3N}$$
$$+ \frac{(A-a)!((A-3)!(a-2)! - (A-2)!(a-3)!)}{(A-3)!(A-2)!}$$
$$\sum_{i_1 < \ldots < i_a = 1}^A \mathcal{V}_{\text{eff},i_1\ldots i_a}^{A,a,NN} \quad (18)$$

then fulfills the constraints for our effective interaction. Specifically for $a = 3$, we get

$$\mathcal{H}_{\text{eff}}^A = \sum_{i=1}^A \left(\frac{\vec{p}_i^{\,2}}{2m_i} + \frac{m_i\Omega^2}{2}\vec{r}_i^{\,2} \right)$$
$$+ \sum_{i_1 < \ldots < i_a = 1}^A \mathcal{V}_{\text{eff},i_1\ldots i_a}^{A,a,3N}$$
$$+ \frac{3-A}{A-2} \sum_{i_1 < \ldots < i_a = 1}^A \mathcal{V}_{\text{eff},i_1\ldots i_a}^{A,a,NN}. \quad (19)$$

This interaction will be used in the calculations in the next section. It will enhance the convergence so that we can obtain meaningful binding energies for p-shell nuclei. In the following, we also use the $a = 3$ approximation, when only "bare" NN forces are taken into account, i.e., when $V_{ijk} = 0$.

We note that the a-body cluster problem is solved in Jacobi coordinates, so that translational invariance of the interaction is guaranteed. The A-body shell model calculation can be done more effectively using a basis of Slater determinants. The transformation from the Jacobi basis to Slater determinants is described in Appendix B.

IV. RESULTS

The main subject of this section is a careful analysis of the numerical accuracy and convergence properties of the results. The cluster approximation induces a sizable Ω dependence, which is driven by the mismatch of the long range behavior of the cluster states and the wave function for the nucleus. The former ones being confined by a HO behave like Gaussians, whereas the latter ones decay exponentially for large distances. Because renormalization of the operators is generally weak for the large distances [58], this cannot be corrected by the renormalization of the interaction, but needs to be taken care of by an optimization of the Ω for the problem and by a rather large model space, which includes enough basis states that the tail is also well approximated. Therefore, to get reliable results, calculations for different model spaces have to be performed for a range of Ωs to identify the optimal choice [59].

The model space size is characterized by the maximal number N of HO excitations included. The lowest ^{7}Li HO configuration has four nucleons in the $n = 0$ HO states and three in the $n = 1$ shell. Therefore, the minimal HO energy is $\mathcal{N}_{\min} = 3$. The A-body calculations include states up to $\mathcal{N}_{\max} = \mathcal{N}_{\min} + N$ [60]. In this work, we perform calculations up to $N = 6$, including configurations up to $\mathcal{N}_{\max} = 9$. The calculations were performed in a basis of single particle Slater determinants (m scheme) using the many-Fermion dynamics code [61,62]. Because we employ HO single-particle states and all Slater determinants up to $\mathcal{N}_{\max}$ are included in the model space, the center-of-mass part can be exactly separated at the end. For $N = 6$, the P-space dimension was 663527, requiring approximately 3×10^9 matrix elements for the A-body Hamiltonian. The effective interactions are based on $a = 3$ clusters. For each model space, we include three-body states up to the maximal excitation of three particles in the A-body configurations. For our largest calculation, these are three-body states up to $\mathcal{N}_3 = 9$ and, for the smaller calculations, this number decreases correspondingly. This implies that the effective interactions are different for each model space size. The results for smaller model spaces do not possess upper bound character.

To solve the cluster equation, we use the Lanczos-scheme. The usage of a Jacobi basis for this problem guarantees the translational invariance of the effective interaction. This is also mandatory to exclude unphysical center of mass excitations from the model space, which would also complicate the selection of the proper states $|n\rangle$ for the definition of the ω operator. The cluster equations are solved using the "bare" interactions for Q spaces up to $\mathcal{N}_3 = 48$ for three-body angular momenta up to $J_3 = \frac{7}{2}$ and $\mathcal{N}_3 = 40$ for $J_3 = \frac{9}{2}$ to $\frac{21}{2}$. The largest dimension for the $\mathcal{N}_3 = 9$ P space is 157 for $J_3^\pi = \frac{5}{2}^-$ and three-body isospin $T_3 = \frac{1}{2}$ making the same amount of bound-state solutions necessary in this channel. Altogether, for all channels between $J_3 = \frac{1}{2}$ and $J_3 = \frac{21}{2}$, we required 2352 states. Convergences for the cluster states has been checked using their binding energies. We take the charge dependence of the NN interaction into account by averaging the NN isospin $t = 1$ interactions according to the prescription given in Ref. [63]. This averaging was performed for total isospin $T = 1/2$ ^{7}Li states. All states we discuss here are
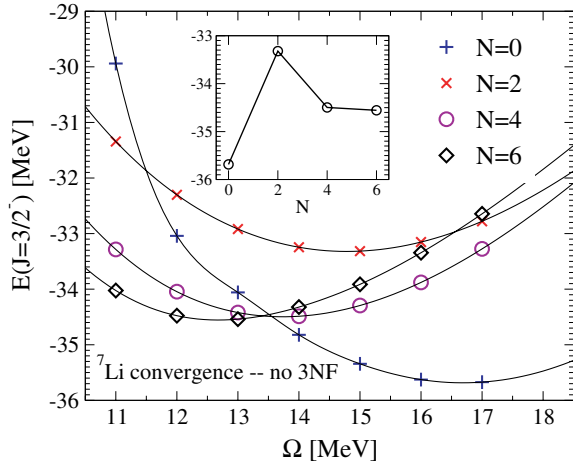
FIG. 3. (Color online) Ω dependence of the binding energy for the ^{7}Li $J^\pi = \frac{3}{2}^-$ ground state using the *NN* interaction only. Results for $N = 0$ to $N = 6$ model spaces are shown.

FIG. 5. (Color online) Ω dependence of the binding energy for the ^{7}Li $J^\pi = \frac{3}{2}^-$ ground state using the *NN* interaction in 3NF-B. Results for $N = 0$ to $N = 6$ model spaces are shown.

$T = 1/2$ states. The Coulomb interaction is not included into the calculation of the effective interaction but is taken into account as an additional "bare" force during the solution of the A-body problem. This does not change any results but will facilitate calculations for $T = 3/2$ states later, which can now be well approximated using the same effective interactions.

In Figs. 3, 4, and 5, we show the Ω dependence of the ground-state binding energy for ^{7}Li with the Idaho-N3LO interaction only and the combinations with 3NF-A and 3NF-B, respectively. The binding energy exhibits a distinct minimum for all model spaces and interactions shown. The position of this minimum shifts to smaller Ω for larger model spaces. This shift becomes smaller for the larger spaces. Also, the position depends on the interaction model. This behavior has been observed for all realistic interactions and makes the extraction of binding energy results more difficult than for the simpler Minnesota type of interactions. Reference [59] investigates this issue in detail. There, it was shown that taking the binding
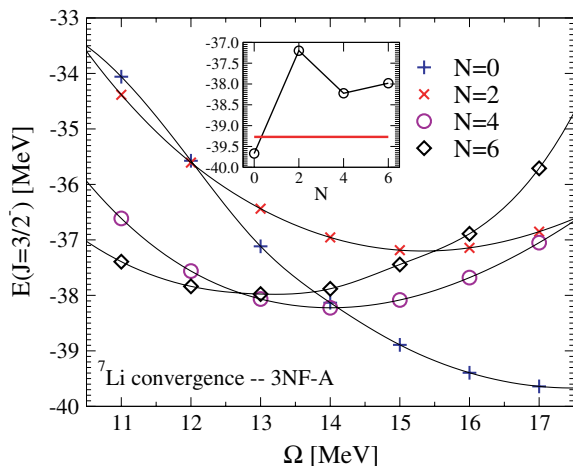
energy of the minimum for different model spaces results in a clear pattern of convergence. It was also shown that the results obtained in this way are consistent with results based on the "bare" interaction. Therefore, we also follow this procedure. The inserts in the figures show the convergence of the binding energy based on this idea for model spaces with $N = 0, 2, 4$, and 6. Very clearly we observe convergence for Idaho-N3LO without 3NF and with 3NF-A. For 3NF-B, the changes in the step $N = 4$ to $N = 6$ are somewhat larger. They are, however, small enough to justify that the results are accurate to the order of the few hundred kiloelectron volts or one megaelectron volts. This will be sufficient for a discussion of the quality of chiral interactions later.

The results for the excitation energies are shown in Figs. 6 to 8. Fortunately, the Ω dependence is rather mild and the different excitation energies are very similar for the $N = 2, 4$, and 6 model spaces. The vertical lines indicate the Ω of the minima for $N = 6$ in Figs. 3 to 5. Our final extraction

FIG. 4. (Color online) Ω dependence of the binding energy for the ^{7}Li $J^\pi = \frac{3}{2}^-$ ground state using the *NN* interaction combined with 3NF-A. Results for $N = 0$ to $N = 6$ model spaces are shown.

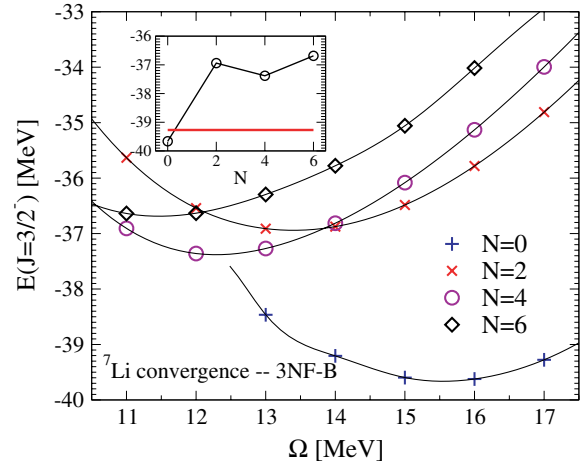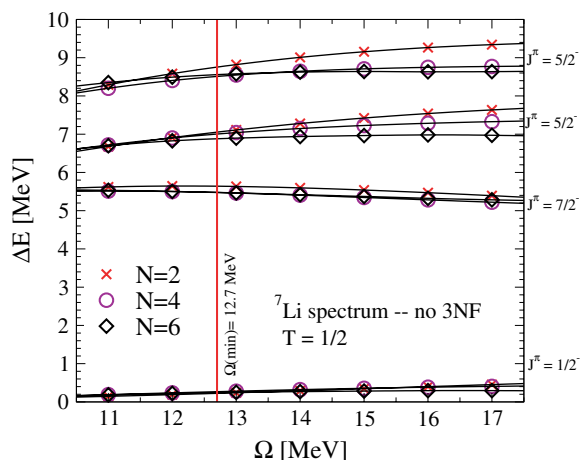FIG. 6. (Color online) Ω dependence of the excitation energy of the lowest states of ^{7}Li using the *NN* interaction only. Results for $N = 0$ to $N = 6$ model spaces are shown.
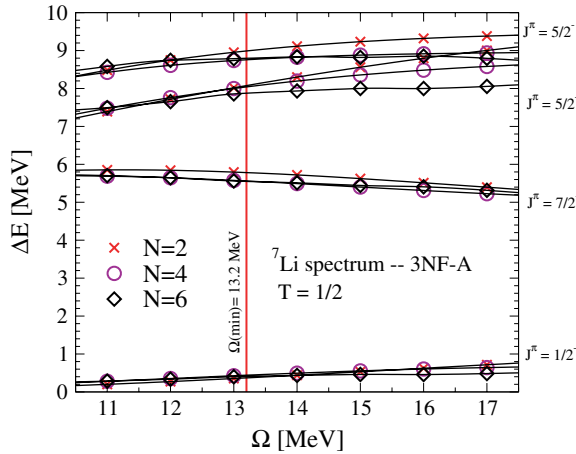
FIG. 7. (Color online) Ω dependence of the excitation energy of the lowest states of ^{7}Li using the *NN* interaction combined with 3NF-A. Results for $N = 0$ to $N = 6$ model spaces are shown.

TABLE III. Comparison of the ground-state binding energy results E_{gs} and the point proton root-mean-square (rms) radius r for ^{7}Li (for $N = 6$ model space and Ω at the minimum of the energy/Ω curve) for chiral interactions and several phenomenological combinations to the experimental value. The experimental rms radius is corrected for the finite size of the proton assuming a proton charge radius of 0.81 fm^{-1}.

Model	E_{gs} (MeV)	r (fm)
NN only	34.6	2.15
w/ 3NF-A	38.0	2.11
w/ 3NF-B	36.7	2.23
AV18 only [7]	31.6	—
AV8'+TM' [65,66]	40.5(1)	2.2(1)
AV18+Urbana IX [7,67]	37.5	2.33
AV18+IL2 [7,67]	38.9	2.25
Expt. [68,69]	39.2	2.27

for the excitation energies is the $N = 6$ result at this Ω value. We also checked the Ω dependence of the binding energy for the excited $1/2^-$ state. Because the position of the minima is very similar to the ones for the $3/2^-$ state, we are confident that the excitation energies for the shown $3/2^-$, $1/2^-$, $7/2^-$, and $5/2^-$ are accurate.

Our results for the binding energy are summarized and compared to other calculations and the experiment in Table III. In addition to our new results, we show results for phenomenological interactions from GFMC calculations. An earlier NCSM results for AV8' and TM' [2] gave 35.8 MeV. It was based only on a single value of $\hbar\Omega$, i.e., 14 MeV, and on three-body cluster states up to $\mathcal{N}_3 = 28$. For a more reliable binding energy prediction, a complete study of the Ω dependence is certainly required as well as an increased number of three-body cluster states. Preliminary results clearly show this trend. Note that we use $\mathcal{N}_3 = 48$ in the present study. Because of this, we omit the earlier NCSM result here and compare to the GFMC results.
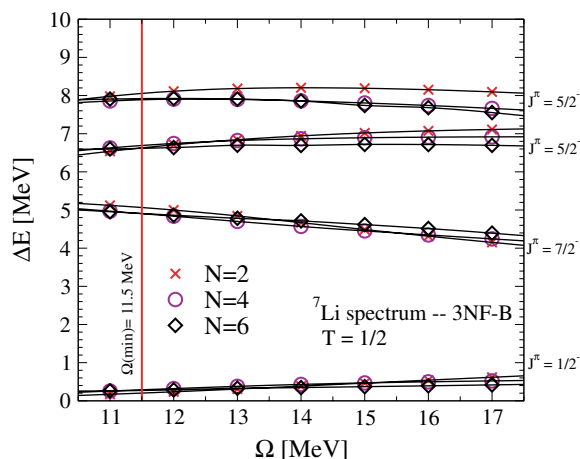
As expected, ^{7}Li is underbound for the *NN* interaction only. Both 3NFs provide more binding. However, in both cases the final binding energy result is still short of the experiment by 1.2 and 2.5 MeV, respectively. In view of the general expectation that strong repulsion at short distances is required to avoid a collapse of nuclei, we are encouraged by the slight underbinding. Clearly, we do not observe any sign of overbinding, though neither the *NN* force nor the 3NF have a strong repulsive core. Both interactions are very soft, yet the binding energies are reasonable. For phenomenogical, pure 2π exchange 3NFs, like the Tucson-Melbourne (TM') [64], overbinding already sets in for ^{7}Li. So far, it was believed that only the addition of a repulsive core, like in the Urbana-IX and Illinois models [7,24], can cure this overbinding problem. Here, we show that the additional structures of chiral 3NFs also prevent overbinding. We note that the description of the binding energy is best for 3NF-A.

The final results for the excitation energies are summarized in Fig. 9. All combinations of the interactions, Idaho-N3LO alone, with 3NF-A or 3NF-B, do predict the right ordering for these states. The splitting of the $3/2^-$ and $1/2^-$ states is small. The agreement with this experimental splitting seems
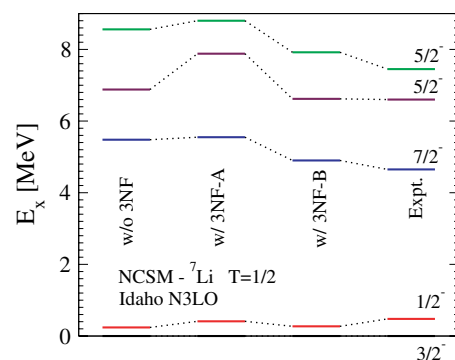

FIG. 8. (Color online) Ω dependence of the excitation energy of the lowest states of ^{7}Li using the *NN* interaction combined with 3NF-B. Results for $N = 0$ to $N = 6$ model spaces are shown.

FIG. 9. (Color online) Dependence of the excitation energy of the lowest states of ^{7}Li on the interaction. Results with the *NN* interaction only and with the 3NF-A and 3NF-B included are compared to the experimental value.
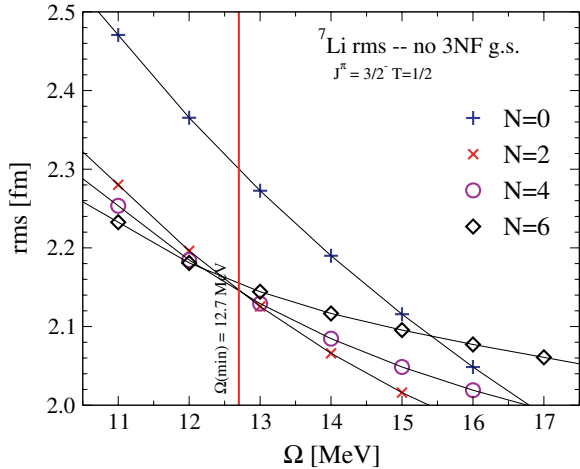
FIG. 10. (Color online) Ω dependence of the point proton rms radius of the ground state of ^{7}Li using the *NN* interaction only. Results for $N = 0$ to $N = 6$ model spaces are shown.

to be superior for 3NF-A. Because the splitting itself is very small, this might be accidental. More significant deviations of the predictions are observed for the $7/2^-$ and $5/2^-$ states. Both, the position of this multiplet and the splitting is strongly affected by the 3NFs and the agreement with the experimental results is clearly best for 3NF-B. This is in contradiction to the binding energy, which was best described for parameter set 3NF-A. For a better clarification of this situation, a study of the dependence on the choice of the c_is is mandatory. This issue is not as simple as it seems at first glance, because the same c_is enter the *NN* interaction. So, in principle, a refitting of the *NN* interaction would be necessary. We postponed this issue to a later study, where this constraint might be loosened to get more insight into the c_i dependence. Finally, we note that part of the deviations for the binding energy might be attributed to our numerical uncertainty. Therefore, the results for ^{7}Li favor the parameter set 3NF-B, because of its superior description of the spectrum, but further calculations will be
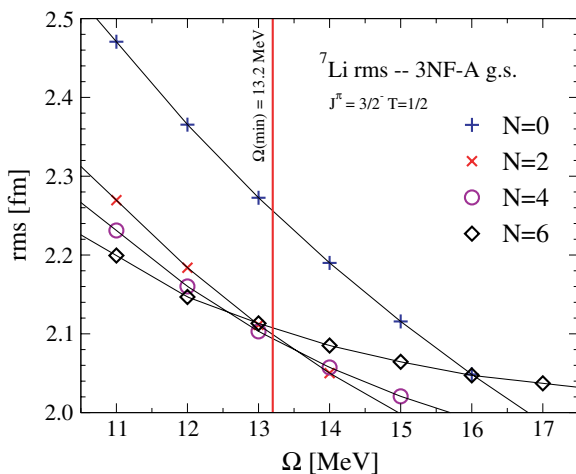

FIG. 11. (Color online) Ω dependence of the point proton rms radius of the ground state of ^{7}Li using the *NN* interaction combined with 3NF-A. Results for $N = 0$ to $N = 6$ model spaces are shown.
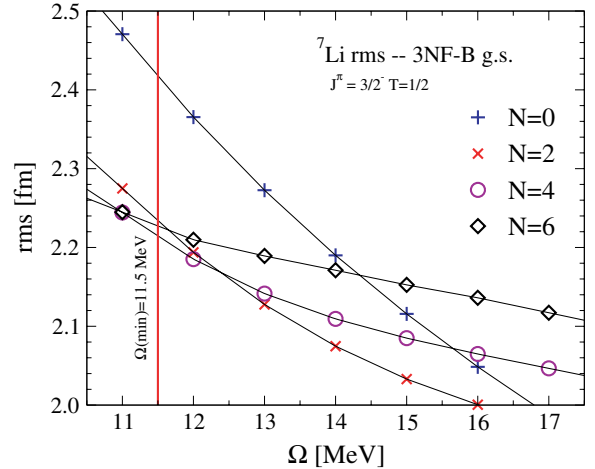

FIG. 12. (Color online) Ω dependence of the point proton rms radius of the ground state of ^{7}Li using the *NN* interaction combined with 3NF-B. Results for $N = 0$ to $N = 6$ model spaces are shown.

required before we can conclude that this result also holds for heavier nuclei.

As discussed, we consider one main result of this first calculation to be that the very soft chiral interactions do not predict a collapse of nuclei with increasing number of nucleons. Of course, this also needs to be confirmed for the densities. Therefore, we also show results for the point proton radii for the $3/2^-$ state in Figs. 10 to 12. For this quantity, we found an interesting dependence on Ω and N. For all model spaces, the radii decrease with increasing Ω. This exactly reflects the behavior of the basis HO states. Obviously, there is no correlation to the binding energy result. It is comforting to note that the slope of this dependence decreases with increasing N. Also, we observed the smallest dependence on N for the Ω values around the minima of the binding energy curves, which are again indicated by vertical lines. Therefore, we have good indications that the best extraction of the radii are obtained for exactly these Ω values for the largest possible model spaces.

Table III also shows the radii obtained in this way and compares them to the experimental values and other calculations. We obtain very realistic results for the chiral interactions, which are comparable to the phenomenological models Urbana-IX, Illinois, and TM'. We do not find any indication that soft, chiral interactions fail to saturate nuclear systems with a realistic binding energy and density. We note that for 3NF-B we even observe an increase of the radius though it provides additional attraction.

V. CONCLUSIONS

We have presented the first microscopic calculation of the low-lying ^{7}Li states based on a full chiral interaction, including *NN* and $3N$ forces. Our results are based on the NCSM. We showed that predictions are possible with an accuracy that allows one to discuss the basic properties of the nuclear force. The results confirm that binding energies and spectra depend on the structure of the 3NFs. This means that the results for

different sets of parameters for the 3NF are different though both models describe the ^{3}H and ^{4}He nuclei with the same accuracy. In this first application, we restricted ourselves to changes in the strength of the short range, or short-range long range pieces (D and E terms) of the 3NF, which are not related to the *NN* interaction at the order Q^3. With this constraint, we have already obtained reasonable results for both, the binding energies and the spectra, but we could not describe both simultaneously within the accuracy, which we expect from our many-body method.

However, we know that the strength of 2π exchange in the *NN* and $3N$ interactions is not well determined yet. Therefore, it is necessary to establish a measure for the dependence of the ^{7}Li and other *p*-shell results on this strength. Because, in principle, this can only be done by changing the *NN* and $3N$ forces, it is not a straightforward and simple task and, probably, for first estimates, one will need to loosen the strict consistency of *NN* and $3N$ forces somewhat. This will be the subject of a forthcoming study.

Here, we were mainly interested to establish that soft chiral interactions result in realistic binding energies and densities. We therefore also investigated the point proton radii and described how these can be extracted from NCSM wave functions. The results support that soft, low-momentum interactions predict reasonable binding energies and densities. In the future, this conjecture needs to be confirmed for heavier systems. In this respect, a study of ^{10}B is a high priority. Results employing the TM' 3NF and the AV8' *NN* force indicate an increasing overbinding going from $A = 7$ to $A = 10$ [65]. It needs to be confirmed that the chiral interactions can again avoid overbinding. At the same time, ^{10}B has proven to be very sensitive to the spin-orbit interactions, including the 3NFs. Usual *NN* interactions, such as Idaho-N3LO and AV18 [2,7,59], predict a wrong ordering of the 3^+ ground and 1^+ excited state. The Illinois type of 3NFs correctly change this ordering and also the TM' 3NF affects this positively, in contrast to the Urbana IX 3NF. Therefore, the predictions of the complete chiral interaction with the 3NF are especially interesting for this nucleus. But also for this system, the dependence on the c_is of the 2π exchange should be studied.

APPENDIX A: EXPLICIT EXPRESSIONS FOR THE CHIRAL 3NFs

In this appendix, we summarize the explicit form of the chiral 3NF. The explicit expressions were first derived in Ref. [44]. The 3NF consists of terms with the three different topologies. The first one is the usual 2π exchange. The operator structure is identical to the well-known Tucson-Melbourne interaction [25]. Then there are two new topologies, which also contain contact interactions (see, e.g., Ref. [18]). In the original work, five independent terms with such structures are derived. In Ref. [18], it was realized that the number of independent terms is smaller once the antisymmetry of the $3N$ states is taken into account. Then only one term of the 1π exchange type (D term) and one term of the pure contact type (E term) are independent.

Following the notation of Ref. [70], the 2π exchange part reads

$$V_{ijk}^{(k);2\pi} = \sum_{i \neq j \neq k} \frac{1}{2} \left(\frac{g_A}{2F_\pi} \right)^2$$
$$\times \frac{(\vec{\sigma}_i \times \vec{q}_j)(\vec{\sigma}_j \times \vec{q}_j)}{\left(\vec{q}_i^2 + m_\pi^2 \right) \left(\vec{q}_j^2 + m_\pi^2 \right)} F_{ijk}^{\alpha\beta} \tau_i^\alpha \tau_j^\beta, \quad \text{(A1)}$$

where $\vec{q}_i$ is the momentum of the pion exchanged between nucleons i and k and

$$F_{ijk}^{\alpha\beta} = \delta^{\alpha\beta} \left[-\frac{4c_1 m_\pi^2}{F_\pi^2} + \frac{2c_3}{F_\pi^2} \vec{q}_i \times \vec{q}_j \right]$$
$$+ \sum_\gamma \frac{c_4}{F_\pi^2} \epsilon^{\alpha\beta\gamma} \tau_k^\gamma \vec{\sigma}_k \times [\vec{q}_i \times \vec{q}_j]. \quad \text{(A2)}$$

The strength of these terms is completely determined by the c_i constants discussed in the main text. The two new terms read

$$V_{ijk}^{(k);1\pi} = -\sum_{i \neq j \neq k} \frac{g_A}{8F_\pi^2} \frac{c_D}{F_\pi^2 \Lambda_\chi} \frac{\vec{\sigma}_j \times \vec{q}_j}{\vec{q}_j^2 + m_\pi^2} (\tau_i \cdot \tau_j)(\vec{\sigma}_i \times \vec{q}_j) \quad \text{(A3)}$$

and

$$V_{ijk}^{(k);\text{cont}} = \frac{1}{2} \sum_{i \neq j \neq k} \frac{c_E}{F_\pi^4 \Lambda_\chi} (\tau_j \cdot \tau_k). \quad \text{(A4)}$$

In these terms two new strength constants c_D and c_E appear. The values, which we determine as described in the main text from the binding energies of ^{3}H and ^{4}He, are based on the choice $\Lambda_\chi = 700$ MeV. For the axial vector coupling constant, we use $g_A = 1.29$. $F_\pi = 92.4$ MeV is the weak pion decay constant and $m_\pi = 138.03$ MeV the averaged pion mass. As outlined in Ref. [18], we regularize the 3NF using a cutoff. Throughout this article, we fix the cutoff to $\Lambda = 500$ MeV.

APPENDIX B: TRANSFORMATION FROM JACOBI TO *M*-SCHEME BASIS

This appendix describes how to transform the effective 3NF from a Jacobi to an *m*-scheme basis.

The effective 3NF is expanded in three-body antisymmetrized Jacobi states [71] with total HO quantum number N, angular momentum J, and isospin T for the internal motion of the three-body cluster. i labels the state within the set of antisymmetrized states with fixed N, J, and T

$$|NJTi\rangle. \tag{B1}$$

This state can be presented in non-anti-symmetrized Jacobi states

$$|\alpha\rangle = |n_{12}n_3[(l_{12}s_{12})j_{12}(l_3 1/2)I_3]JM_J(t_{12}1/2)TM_T\rangle \tag{B2}$$

using coefficients of fractional parentage (CFP)

$$c_{\alpha i} = \langle \alpha|NJTi\rangle. \tag{B3}$$

We obtain the c_i by diagonalizing the antisymmetrizer in the Jacobi basis $|\alpha\rangle$ [71].

The single particle m-scheme states are

$$|abc\rangle = \left|n_a(l_a 1/2)j_a m_a m_a^t\right\rangle \left|n_b(l_b 1/2)j_b m_b m_b^t\right\rangle$$
$$\left|n_c(l_c 1/2)j_c m_c m_c^t\right\rangle. \tag{B4}$$

We do not need to explicitly antisymmetrize these states, because we project on antisymmetrized Jacobi states in the following. This implies that for all orderings of a, b, and c the transformation matrix element will be the same.

The internal motion is augmented by c.m. HO basis states $|n_{\text{c.m.}}l_{\text{c.m.}}\rangle$, which we couple with the states for the intrinsic motion to a total angular momentum $\mathcal{J}\mathcal{M}$

$$\{|n_{\text{c.m.}}l_{\text{c.m.}}\rangle|NJTi\rangle\}^{\mathcal{J}\mathcal{M}}. \tag{B5}$$

Analogously, the states $|\alpha\rangle$ are augmented by C.M. states. Note that the CFP's are m independent. Therefore, the CFPs are identical in the complete and in the internal basis

$$c_{\alpha i} = \{\langle n_{\text{c.m.}}l_{\text{c.m.}}|\langle\alpha|\}^{\mathcal{J}\mathcal{M}}\{|n_{\text{c.m.}}l_{\text{c.m.}}\rangle|NJTi\rangle\}^{\mathcal{J}\mathcal{M}}. \tag{B6}$$

It is efficient to also couple the single-particle states to a total angular momentum $\mathcal{J}\mathcal{M}$, because the transformation conserves the total angular momentum. We introduce the intermediate angular momentum J_{12} and define

$$\{\{|a\rangle|b\rangle\}^{J_{12}}|c\rangle\}^{\mathcal{J}\mathcal{M}}. \tag{B7}$$

The noncoupled states are easily projected out of the coupled ones using orthogonality relations of the Clebsch-Gordan coefficients

$$\langle abc|\{\{|a\rangle|b\rangle\}^{J_{12}}|c\rangle\}^{\mathcal{J}\mathcal{M}} = (j_a j_b J_{12}, m_a m_b m_a + m_b)$$
$$\times (J_{12}j_c\mathcal{J}, m_a + m_b m_c \mathcal{M}). \tag{B8}$$

In this notation the transformation of the Jacobi basis matrix elements of the 3NF $\langle NJTi|V_3|NJTi\rangle$ reads

$$\langle abc|V_3|a'b'c'\rangle = \sum_{\mathcal{J}J_{12}J_{12}'}\sum_{\alpha\alpha'}\sum_{ii'}$$
$$\times (j_a j_b J_{12}, m_a m_b m_a + m_b)$$
$$\times (J_{12}j_c\mathcal{J}, m_a + m_b m_c m_a + m_b + m_c)$$
$$\times (j_a' j_b' J_{12}', m_a' m_b' m_a' + m_b')$$
$$\times (J_{12}' j_c'\mathcal{J}, m_a' + m_b' m_c' m_a' + m_b' + m_c')$$
$$\times \{\{\langle a|\langle b|\}^{J_{12}}\langle c|\}^{\mathcal{J}}\{|n_{\text{c.m.}}l_{\text{c.m.}}\rangle|\alpha\rangle\}^{\mathcal{J}}$$
$$\times c_{\alpha i}c_{\alpha' i'}\langle NJTi|V_3|NJTi\rangle$$
$$\times \{\langle n_{\text{c.m.}}l_{\text{c.m.}}|\langle\alpha'|\}^{\mathcal{J}}\{\{|a'\rangle|b'\rangle\}^{J_{12}'}|c'\rangle\}^{\mathcal{J}}. \tag{B9}$$

Here, we made use of the orthogonality of the Clebsch-Gordan coefficients, which removed the m-sums and resulted in $\mathcal{J} = \mathcal{J}'$. The transition matrix element

$$T = \{\langle n_{\text{c.m.}}l_{\text{c.m.}}|\langle\alpha|\}^{\mathcal{J}}\{\{|a\rangle|b\rangle\}^{J_{12}}|c\rangle\}^{\mathcal{J}} \tag{B10}$$

becomes $\mathcal{M}$ independent. The spin-orbital part is then obtained as

$$T = \sum_{\mathcal{L}_{12}S_3 L_3 L_{12}\mathcal{L}\Lambda}\sqrt{\hat{j}_{12}\hat{I}_3\hat{L}_3\hat{S}_3}\begin{Bmatrix} l_{12} & l_3 & L_3 \\ s_{12} & 1/2 & S_3 \\ j_{12} & I_3 & J \end{Bmatrix}$$

$$\times (-)^{L_3+S_3+l_{\text{c.m.}}+\mathcal{J}}\sqrt{\hat{\mathcal{L}}\hat{\mathcal{J}}}\begin{Bmatrix} l_{\text{c.m.}} & L_3 & \mathcal{L} \\ S_3 & \mathcal{J} & J \end{Bmatrix}\sqrt{\hat{L}_{12}\hat{s}_{12}\hat{j}_a\hat{j}_b}$$

$$\times \begin{Bmatrix} l_a & l_b & L_{12} \\ 1/2 & 1/2 & s_{12} \\ j_a & j_b & J_{12} \end{Bmatrix}\sqrt{\hat{J}_{12}\hat{j}_c\hat{\mathcal{L}}\hat{S}_3}\begin{Bmatrix} L_{12} & s_{12} & J_{12} \\ l_c & 1/2 & j_c \\ \mathcal{L} & S_3 & \mathcal{J} \end{Bmatrix}$$

$$\times (-)^{l_{12}+l_3-L_3}(-)^{l_{\text{c.m.}}+l_3+l_{12}+\mathcal{L}}\sqrt{\hat{\Lambda}\hat{L}_3}\begin{Bmatrix} l_{\text{c.m.}} & l_3 & \Lambda \\ l_{12} & \mathcal{L} & L_3 \end{Bmatrix}$$

$$\times (-)^{\mathcal{L}_{12}+l_c-\Lambda}(-)^{l_c+L_{12}-\mathcal{L}}(-)^{l_c+l_{12}+\mathcal{L}_{12}+\mathcal{L}}\sqrt{\hat{\Lambda}\hat{L}_{12}}$$

$$\times \begin{Bmatrix} l_c & \mathcal{L}_{12} & \Lambda \\ l_{12} & \mathcal{L} & L_{12} \end{Bmatrix}[n_{\text{c.m.}}l_{\text{c.m.}}, n_3 l_3 : \Lambda; N_{12}\mathcal{L}_{12}, n_c l_c : \Lambda]_d$$

$$\times [N_{12}\mathcal{L}_{12}, n_{12}l_{12} : L_{12}; n_a l_a, n_b l_b : L_{12}]_{d'} \tag{B11}$$

using the Talmi-Moshinsky brackets with $d = 2$ and $d' = 1$ (for the notation see Ref. [72]). For the isospin matrix element, one finds

$$T_{\text{iso}} = (1/2\,1/2\,t_{12}, m_a^t m_b^t m_a^t + m_b^t)$$
$$\times (t_{12}\,1/2\,T, m_a^t + m_b^t m_c^t m_a^t + m_b^t + m_c^t). \tag{B12}$$

We note that a simpler expression for this transformation was derived in Ref. [2]. The present formula is, however, more efficient.

[1] S. C. Pieper and R. B. Wiringa, Annu. Rev. Nucl. Part. Sci. **51**, 53 (2001).

[2] P. Navrátil and E. W. Ormand, Phys. Rev. C **68**, 034305 (2003).

[3] V. G. J. Stoks, R. A. M. Klomp, C. P. F. Terheggen, and J. J. de Swart, Phys. Rev. C **49**, 2950 (1994).

[4] R. B. Wiringa, V. G. J. Stoks, and R. Schiavilla, Phys. Rev. C **51**, 38 (1995).

[5] R. Machleidt, F. Sammarruca, and Y. Song, Phys. Rev. C **53**, R1483 (1996).

[6] R. Machleidt, Phys. Rev. C **63**, 024001 (2001).

[7] S. C. Pieper, V. R. Pandharipande, R. B. Wiringa, and J. Carlson, Phys. Rev. C **64**, 14001 (2001).

[8] T.-S. Park, L. E. Marcucci, R. Schiavilla, M. Viviani, A. Kievsky, S. Rosati, K. Kubodera, D.-P. Min, and M. Rho, Phys. Rev. C **67**, 055206 (2003).

[9] V. Bernard, N. Kaiser, and U.-G. Meißner, Int. J. Mod. Phys. E **4**, 193 (1995).

[10] U. van Kolck, Prog. Part. Nucl. Phys. **43**, 337 (1999).

[11] P. F. Bedaque and U. van Kolck, Annu. Rev. Nucl. Part. Sci. **52**, 339 (2002).

[12] E. Epelbaum, accepted for publication in Prog. Part. Nucl. Physics, nucl-th/0509032.

[13] H. Witała, W. Glöckle, J. Golak, A. Nogga, H. Kamada, R. Skibiński, and J. Kuroś-Żołnierczuk, Phys. Rev. C **63**, 24007 (2001).

[14] R. Bieber, W. Glöckle, J. Golak, M. N. Harakeh, D. Hüber, H. Huisman, N. Kalantar-Nayestanaki, H. Kamada, J. G. Messchendorp, A. Nogga *et al.*, Phys. Rev. Lett. **84**, 606 (2000).

[15] H. Sakai, K. Sekiguchi, H. Witała, W. Glöckle, M. Hatano, H. Kamada, H. Kato, Y. Maeda, A. Nogga, T. T. Ohnishi *et al.*, Phys. Rev. Lett. **84**, 5288 (2000).

[16] R. V. Cadman, J. Brack, W. J. Cummings, J. A. Fedchak, B. D. Fox, H. Gao, W. Glöckle, J. Golak, C. Grosshauser, R. J. Holt *et al.*, Phys. Rev. Lett. **86**, 967 (2001).

[17] K. Ermisch, A. M. van den Berg, R. Bieber, W. Glöckle, J. Golak, M. Hagemann, V. M. Hannen, M. N. Harakeh, M. A. de Huu, N. Kalantar-Nayestanaki *et al.*, Phys. Rev. Lett. **86**, 5862 (2001).

[18] E. Epelbaum, A. Nogga, W. Glöckle, H. Kamada, U.-G. Meißner, and H. Witała, Phys. Rev. C **66**, 064001 (2002).

[19] W. Polyzou and W. Glöckle, Few-Body Syst. **9**, 97 (1990).

[20] P. Navrátil, J. P. Vary, and B. R. Barrett, Phys. Rev. Lett. **84**, 5728 (2000).

[21] P. Navrátil, J. P. Vary, and B. R. Barrett, Phys. Rev. C **62**, 54311 (2000).

[22] A. Nogga, H. Kamada, W. Glöckle, and B. R. Barrett, Phys. Rev. C **65**, 054003 (2002).

[23] P. Navrátil and B. R. Barrett, Phys. Rev. C **57**, 3119 (1998).

[24] B. S. Pudliner, V. R. Pandharipande, J. Carlson, S. C. Pieper, and R. B. Wiringa, Phys. Rev. C **56**, 1720 (1997).

[25] S. A. Coon, M. D. Scadron, P. C. McNamee, B. R. Barrett, D. W. E. Blatt, and B. H. J. McKellar, Nucl. Phys. **A317**, 242 (1979).

[26] E. Braaten and H. W. Hammer, Phys. Rept. **428**, 259 (2006); cond-mat/0410417.

[27] L. Platter, H. W. Hammer, and U.-G. Meißner, Phys. Lett. **B607**, 254 (2005).

[28] S. Weinberg, Physica A **96**, 327 (1979).

[29] N. Fettes, U.-G. Meißner, and S. Steininger, Phys. Lett. **B451**, 233 (1999).

[30] U. van Kolck, J. L. Friar, and T. Goldman, Phys. Lett. **B371**, 169 (1996).

[31] S. Weinberg, Phys. Lett. **B251**, 288 (1990).

[32] S. Weinberg, Nucl. Phys. **B363**, 3 (1991).

[33] S. Weinberg, Phys. Lett. **B295**, 114 (1992).

[34] C. Ordóñez, L. Ray, and U. van Kolck, Phys. Rev. C **53**, 2086 (1996).

[35] E. Epelbaum, W. Glöckle, and U.-G. Meißner, Nucl. Phys. **A671**, 295 (2000).

[36] D. R. Entem and R. Machleidt, Phys. Lett. **B524**, 93 (2002).

[37] D. R. Entem and R. Machleidt, Phys. Rev. C **68**, 041001(R) (2003).

[38] E. Epelbaum, W. Glöckle, and U.-G. Meißner, Nucl. Phys. **A747**, 362 (2005).

[39] D. B. Kaplan, M. J. Savage, and M. B. Wise, Phys. Lett. **B424**, 390 (1998).

[40] S. Fleming, T. Mehen, and I. W. Stewart, Nucl. Phys. **A677**, 313 (2000).

[41] P. Büttiker and U.-G. Meißner, Nucl. Phys. **A668**, 97 (2000).

[42] M. C. M. Rentmeester, R. G. E. Timmermans, and J. J. de Swart, Phys. Rev. C **67**, 044001 (2003).

[43] R. A. M. Klomp, V. G. J. Stoks, and J. J. de Swart, Phys. Rev. C **44**, R1258 (1991).

[44] U. van Kolck, Phys. Rev. C **49**, 2932 (1994).

[45] N. Fettes, U.-G. Meißner, and S. Steininger, Nucl. Phys. **A640**, 199 (1998).

[46] M. C. M. Rentmeester, R. G. E. Timmermans, J. L. Friar, and J. J. de Swart, Phys. Rev. Lett. **82**, 4992 (1999).

[47] K. Suzuki and S. Y. Lee, Prog. Theor. Phys. **64**, 2091 (1980).

[48] K. Suzuki, Prog. Theor. Phys. **68**, 246 (1982).

[49] S. Okubo, Prog. Theor. Phys. **12**, 603 (1954).

[50] E. Epelbaoum, W. Glöckle, and U.-G. Meißner, Nucl. Phys. **A637**, 107 (1998).

[51] E. Epelbaoum, W. Glöckle, A. Krüger, and U.-G. Meißner, Nucl. Phys. **A645**, 413 (1998).

[52] S. K. Bogner, T. T. S. Kuo, and A. Schwenk, Phys. Rep. **386**, 1 (2003).

[53] N. Barnea, W. Leidemann, and G. Orlandini, Phys. Rev. C **61**, 54001 (2000).

[54] N. Barnea, W. Leidemann, and G. Orlandini, Nucl. Phys. **A693**, 565 (2001).

[55] H. J. Lipkin, Phys. Rev. **109**, 2071 (1958).

[56] P. Navrátil and B. R. Barrett, Phys. Rev. C **54**, 2986 (1996).

[57] C. P. Viazminsky and J. P. Vary, J. Math. Phys. **42**, 2055 (2001).

[58] I. Stetcu, B. R. Barrett, P. Navrátil, and J. P. Vary, Phys. Rev. C **71**, 044325 (2005).

[59] P. Navrátil and E. Caurier, Phys. Rev. C **69**, 014311 (2004).

[60] Note that in previous works, what we call N here was labeled "$N_{\rm max}$."

[61] J. P. Vary (unpublished).

[62] J. P. Vary and D. C. Zheng (unpublished).

[63] G. P. Kamuntavičius, P. Navrátil, B. R. Barrett, G. Sapragonaite, and R. K. Kalinauskas, Phys. Rev. C **60**, 044304 (1999).

[64] S. A. Coon and H. K. Han, Few-Body Syst. **30**, 131 (2001).

[65] S. C. Pieper, Nucl. Phys. **A751**, 516c (2005).

[66] S. C. Pieper (private communication).

[67] S. C. Pieper, R. B. Wiringa, and J. Carlson, Phys. Rev. C **70**, 054325 (2004).

[68] D. R. Tilley, C. M. Cheves, J. L. Godwin, G. M. Hale, H. M. Hofmann, J. H. Kelley, C. G. Shen, and H. R. Weller, Nucl. Phys. **A708**, 3 (2002).

[69] H. de Vries, C. W. de Jager, and C. de Vries, At. Data Nucl. Data Tables **36**, 495 (1987).

[70] J. L. Friar, D. Hüber, and U. van Kolck, Phys. Rev. C **59**, 53 (1999).

[71] P. Navrátil, G. P. Kamuntavicius, and B. R. Barrett, Phys. Rev. C **61**, 44001 (2000).

[72] G. P. Kamuntavicius, R. K. Kalinauskas, B. R. Barrett, S. Mickevičius, and D. Germanas, Nucl. Phys. **A695**, 191 (2001).